American Mineralogist, Volume 83, pages 1357–1360, 1998

Ultrasonic interferometry and X-ray measurements on MgO in a new diamond anvil cell

H.J. REICHMANN,[1,*] R.J. ANGEL,[1] H. SPETZLER,[2] AND W.A. BASSETT[3]

[1]Bayerisches Geoinstitut, Universitaet Bayreuth, D-95440 Bayreuth, Germany
[2]Department of Geological Sciences and CIRES, University of Colorado, Boulder, Colorado 80309, U.S.A.
[3]Department of Geological Sciences, Cornell University, Ithaca, New York 14853, U.S.A.

ABSTRACT

The compressional sound wave velocity, v_p, of synthetic MgO in the (100) direction and the unit-cell parameter have been measured up to a maximum pressure of 6.1 GPa using a new type of diamond-anvil cell. The main feature of the cell is the transverse access of the X-ray beam into the sample chamber. This allows us to undertake single crystal X-ray measurements while the ultrasonic attachment is mounted on the diamond-anvil cell. The sound velocity and the elastic parameter c_{11} have been determined from these measurements; the variation with pressure can be described by $\partial c_{11}/\partial p = 9.35(13)$, in good agreement with previous studies.

INTRODUCTION

Our knowledge of the Earth's structure is based upon seismological data. Comparison between laboratory data and seismological data can provide information about the chemistry and mineralogy of Earth's interior.

Silicate perovskite and (Mg,Fe)O are likely to be important constituents of the lower mantle (e.g., Anderson 1989). Because of its wide stability field and its simple rocksalt structure the elastic properties of the end-member periclase (MgO) have been examined intensively in experimental and theoretical studies (e.g., Jackson and Niesler 1982; Duffy et al. 1995; Karki et al. 1997; Chopelas 1992; Chen et al. 1997; Chen et al. 1998). Moreover, although MgO is cubic and therefore optically isotropic, it shows a large elastic anisotropy of about 10% between the [100] and [111] directions at ambient conditions (Jackson and Niesler 1982).

In the following we report measurements of the pressure derivative of the elastic constant in the (100) direction and the unit-cell parameter of MgO under high pressures. The experiments were performed in a newly built diamond-anvil cell, which enables us to perform ultrasonic interferometry and single crystal X-ray measurements simultaneously.

EXPERIMENTAL METHODS

Cylindrical MgO (100) samples, which were oriented with an accuracy of 0.5°, were cut from a synthetic, clean single crystal obtained from Roditi, Hamburg. The thicknesses of the samples we used in the DAC ranged from about 60 to 150 μm, their diameters were between 200 to 250 μm. The MgO pieces were polished optically flat on both sides to obtain good ultrasonic echoes from the sample.

New diamond-anvil cell

The requirements for X-ray diffraction and ultrasonic measurements in a DAC are very different. For successful high precision measurement of unit-cell parameters a wide angular access to the sample by X-rays is required. By contrast, the ultrasonic signals must be transmitted to the sample through one of the diamonds by means of a buffer rod and associated potentially bulky alignment mechanism. To be able to perform ultrasonic and X-ray measurements we built a new diamond-anvil cell with only two guide rods. The main feature of this new cell is the transverse access of the X-ray beam to the sample (Fig. 1). The upper and lower platen provide an opening angle of approximately 65°on each side, and the two support rods provide an access angle of about 120° on each side of the DAC in the equatorial plane. Although this cell has only two guide rods and therefore does not have the stability compared to more conventional cell designs with three or more posts (e.g., Merrill and Bassett 1974; Allan et al. 1995) we reached a pressure of 6.1 GPa using diamond culets of 0.6 mm. Using culets of 0.5 mm diameter a pressure range of 9–10 GPa should be achievable. Stainless steel gaskets with initial thicknesses of 250 μm were used.

Further, the cell can be heated through molybdenum wires 0.25 mm in diameter wound around the tungsten carbide diamond seats, and temperature can be measured by K-type thermocouples fixed directly onto the two diamond anvils. For X-ray diffraction measurements the cell is attached to a modified x-y goniometer head by four ceramic posts (for heat insulation) and an intermediate steel plate to act as a heat shield. Because this attachment is made via the lower platen of the cell, the buffer rod can be left in place during diffraction measurements, and ultrasonic measurements can be made while the cell is mounted on the single-crystal X-ray diffractometer (Fig. 2).

Ultrasonics

The technique of ultrasonic interferometry measurements (Spetzler et al. 1993) has been adopted for use in the diamond-anvil cell (Spetzler et al. 1996). Briefly, ultrasonic signals from a 1.5 μm thin ZnO transducer are introduced to the sample by means of single-crystal sapphire rod (cut with its long axis parallel to c) which is pressed against the table face of the dia-

*E-mail: hans-josef.reichmann@uni-bayreuth.de

0003-004X/98/1112–1352$05.00

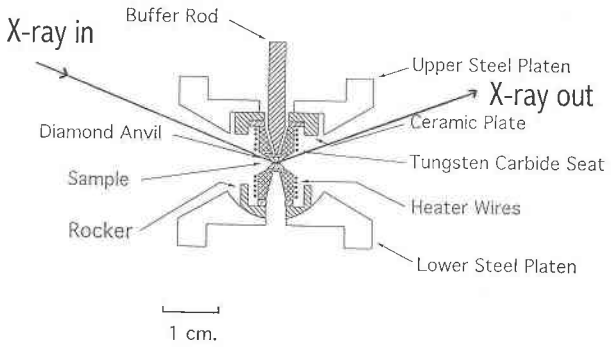

FIGURE 1. A sketch of the new geometry of the diamond-anvil cell. The important feature is the wide transverse opening angle for the X-ray measurements.

mond anvil carrying the sample (Fig. 3). Travel time measurements of the ultrasonic signals in the sample are made by interfering the signal reflected from the far end of the sample with that reflected from the sample/diamond interface (these reflected sound waves are represented by arrows 2 and 3 in Fig. 3). This interferometric technique eliminates the necessity of measuring the travel times through the buffer rod and diamond, but it is critically dependent upon good energy transfer between the buffer rod and the diamond and between the diamond and the crystal sample.

Each maximum and each minimum in the interference pattern results from constructive and destructive interference, respectively, and thus represents a separate measurement of the travel time, t. The travel time is related to the frequencies, f_m, where the extrema occur through the relationship $t = m/f_m$; where m is the corresponding order of the fringe, i.e., an even multiple of $^1/_2$ for maxima and an odd multiple for minima (for further details see Spetzler et al. 1993).

The MgO sample was adhered to the diamond with super glue to obtain the tight mechanical contact, which is necessary for a good sample echo. To avoid curing effects of the glue, the first travel time measurements were done 24 h after gluing. For our experiments we used samples with different initial thicknesses $d = l/2$, where l is the total path length for the ultrasonic sound waves in the sample.

The ultrasonic technique demands parallel sample faces. The MgO pieces are polished on a 47 mm long glass slide. At the end of the polishing process the thickness difference at the ends of the glass slide is about 3 μm (over a distance of 47 mm), so the calculated thickness difference (= non parallelism of the sample faces) of a sample with 200 μm diameter is about 0.01 μm, which makes a negligible contribution to the uncertainties of the experiments.

To determine the zero pressure thickness we measured the travel time at ambient conditions and calculated the zero pressure thickness according to the relation $d_0 = v_0\, t_0\, /2$, where v_0 = 9100 m/s sound velocity at zero pressure (Jackson and Niesler 1982), d_0 is the sample length at zero pressure and t_0 is the measured zero pressure travel time. The uncertainty of t_0 ranges from 30 to 190 ps with an average of 90 ps, resulting in an uncertainty of l_0 between 0.1 μm and 1.1 μm. This uncertainty is mainly due to the poor

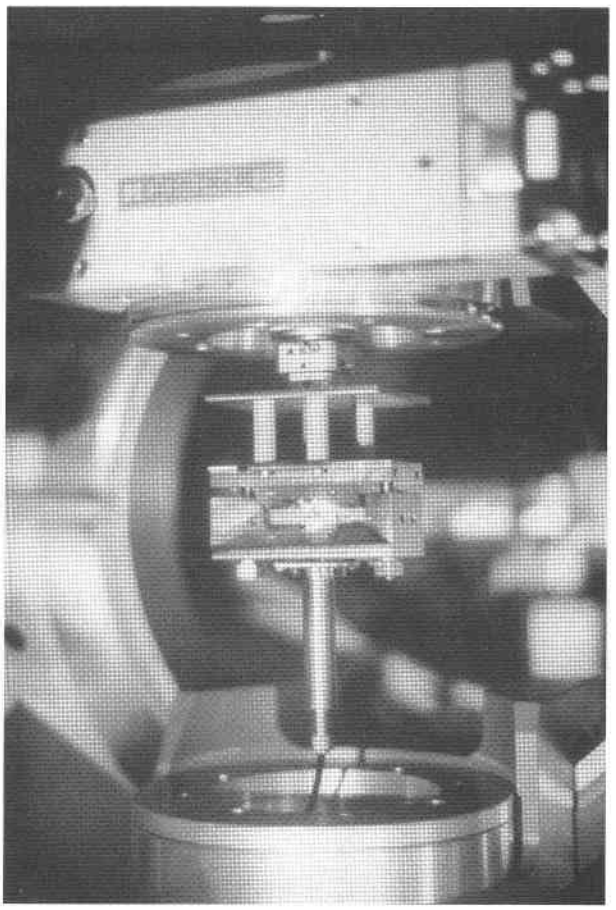

FIGURE 2. The new diamond-anvil cell with the ultrasonic attachment in the four-circle diffractometer.

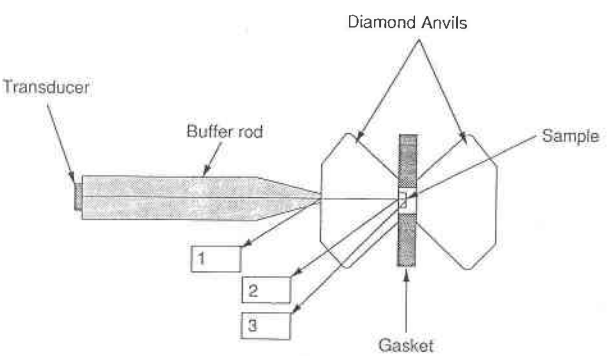

FIGURE 3. Schematic diagram of the buffer rod and the diamond anvils. The ultrasonic sound waves, created by the transducer, propagate through the buffer rod, the diamond and the sample. A part of the energy is reflected at the buffer rod-diamond interface (represented by arrow no. 1), at the diamond-sample interface (no. 2) and at the backside of the sample (no. 3). The overlapping of the last two sound waves gives rise to an interference pattern from which the travel time can be determined.

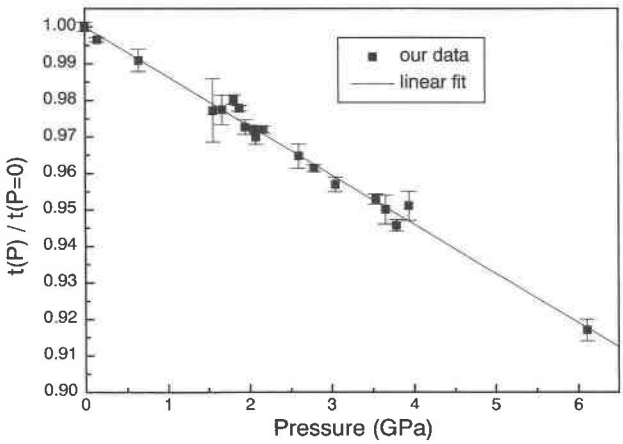

FIGURE 4. Normalized travel time $t(P)/t(P = 0)$ vs. pressure. $t(P)$ is the travel time at high pressure, $t(P = 0)$ travel time at zero pressure. The straight line is a linear fit through the points. The uncertainties in P are smaller than the symbol size.

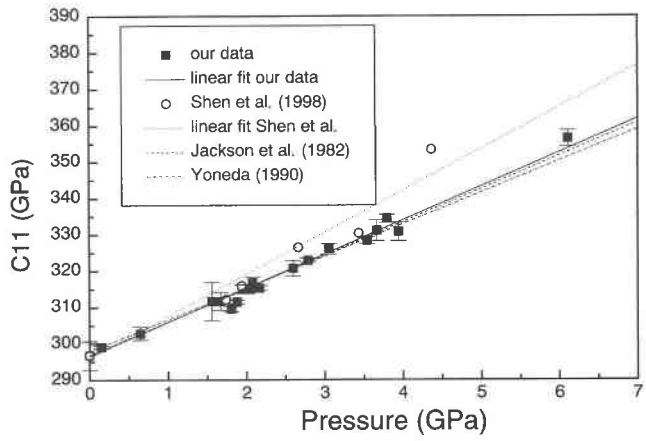

FIGURE 5. The elastic modulus c_{11} as function of pressure. Solid squares are our measurements, the open circles are from the work of Shen et al. (1998). The solid line is a linear fit through our data, the dotted line is a linear fit through Shen et al. (1998) data. The dashed line next to the solid line represents the elastic modulus c_{11} by Jackson and Niesler (1982), the dashed dotted line are the data by Yoneda (1990).

coupling of the MgO slice to the diamond at zero pressure. At high pressure the uncertainty in travel time measurement decreases because of the better coupling of the sample to the diamond and lies between 10 and 100 ps with an average of 50 ps.

The pressure medium was either a 4:1 methanol-ethanol mixture or pure ethanol. The pressure in the sample chamber was measured by means of the ruby fluorescence technique (Piermarini et al. 1975). The thickness d of the cubic MgO changes as a function of pressure P according to $(d(P)/d_0) = [\rho(P)/\rho_0]^{-1/3}$, where ρ is density. The longitudinal sound wave velocity is given by $v(P) = l(P)/t$. The density $\rho(P)$ of MgO was calculated using the third order Birch-Murnaghan EOS.

$$P = \frac{3}{2}\left[\left(\frac{\rho}{\rho_0}\right)^{2/3} - 1\right]\left(\frac{\rho}{\rho_0}\right)^{5/3} K_0\left\{1 + \frac{3}{4}(K_0' - 4)\left[\left(\frac{\rho}{\rho_0}\right)^{2/3} - 1\right]\right\}.$$

The isothermal bulk modulus $K_T = 160.2$ GPa was calculated using the relation $K_S = K_T(1 + \alpha\gamma T)$, with $K_S = 162.5$ GPa (Jackson and Niesler 1982), the thermal expansion coefficient ($= 3.12 \cdot 10^{-6}$ K^{-1} (Anderson et al. 1989) and the Grüneisen parameter $\gamma = 1.54$ (Anderson et al. 1989). K' was taken as 4.09 (Jackson and Niesler 1982).

X-ray

The X-ray measurements were performed with a four-circle diffractometer from Huber, which nominally provides a precision in the volume measurements of 1 part in 10^4 (Angel et al. 1997). However, the precision of the measurements with the new type of diamond-anvil cell used in our experiments is five parts in 10^4 because of the shadowing of the sample due to the gasket. If the sample is much thinner than the gasket then the X-ray beam is partially or completely absorbed by the gasket because of the transverse access of the X-ray beam into the sample chamber. This has the effect that fewer X-ray reflections are detectable and a consequent decrease in precision. When we started these measurements this shadowing effect prohibited us from collecting enough X-ray data to determine bulk modulus K_0 and the derivative K', which we need to determine the sample length. For this reason we used Jackson and Niesler's data (1982) to calculate the sample thickness as a function of pressure.

RESULTS AND DISCUSSION

Figure 4 shows the normalized travel time $t(P)/t(P = 0)$ vs. pressure, with $t(P)$ the travel time at pressure P and $t(P = 0)$ the travel time of the same sample at zero pressure. A linear curve fitted to the data has a regression coefficient of 0.994. The uncertainty in the normalized travel time is due to the uncertainty in the determination of $t(P)$ at high pressure. The uncertainties in pressure determined by means of the ruby fluorescence method are typically 0.05 GPa.

The uncertainties in the elastic constant c_{11} at pressure (Fig. 5) arise from the uncertainties in the determination of the travel time at high pressure. A linear fit of the data yields the relationship $\partial c_{11}/\partial P = 9.35(13)$. Our data agree very well with that of Jackson and Niesler (1982), who examined a single crystal MgO sample in a frequency range of 10 to 80 MHz up to a pressure of 3 GPa, and with the data of Yoneda (1990) who measured MgO up to 7.78 GPa in a frequency range of 40–60 MHz. The excellent matching of these data sets shows that MgO has almost no dispersion in the frequency range from 10 MHz to 2 GHz. Similarly, Sinogeikin et al. (1998) report good agreement between Brillouin scattering measurements of MgO, which have an even higher effective frequency, and ultrasonic data.

The high-pressure elasticity measurements of MgO by Shen et al. (1998) deviate to higher values of c_{11} than the current study (Fig. 5). This disparity is probably due to the fact that Shen et al. (1998) used solid KBr as a pressure medium, which is non-hydrostatic, whereas our measurements were performed with pure ethanol or, at pressures

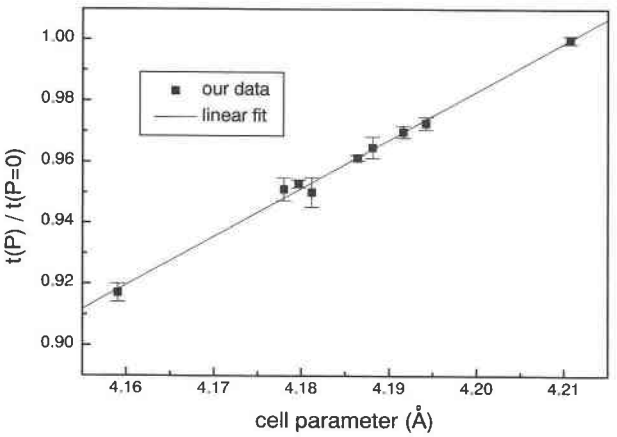

FIGURE 6. Normalized travel time $t(P)/t(P = 0)$ vs. cell parameter. $t(P)$ is the travel time at high pressure, $t(P = 0)$ travel time at zero pressure. The straight line is a linear fit through the points. No ruby pressure measurement is involved in this plot. The uncertainties of the cell parameters are smaller than the symbols.

higher than 3.5 GPa, a 4:1 methanol-ethanol mixture, which is known to be hydrostatic up to 9 GPa (Piermarini et al. 1973).

In Figure 6 the ratio $t(P)/t(P = 0)$ obtained from the ultrasonic measurements is seen to lineraly depend on the cell parameter determined from the X-ray diffraction measurements. The travel time and the corresponding cell parameter are measured under identical conditions, i.e., the pressure remains constant for one pair of measurements. There are fewer data points than in Figure 4 because the shadowing by the gasket precluded X-ray measurements for some sample configurations. The self-consistency of these two measurement methods indicates that this diamond-anvil cell has the potential to exploit the complete travel time EOS of Spetzler and Yoneda (1993) and thereby to determine an absolute pressure scale to high precision.

ACKNOWLEDGMENTS

We wish to express our thanks to G. Herrmannsdoerfer, H. Schulze, and R. Weigel of the Bayerisches Geoinstitut for their extensive technical help with this project. We gratefully acknowledge the support of NATO in the form of a collaborative research grant to R.J.A. and W.A.B., and the Alexander-von-Humboldt Stiftung for a Humboldt Preis to H.S.

REFERENCES CITED

Anderson, D.L. (1989) Theory of the Earth. Blackwell Scientific Publications, Boston, Massachusetts.

Anderson, O.L. and Zou, K. (1989) Formulation of the thermodynamic functions for mantle minerals: MgO as an example. Physics and Chemistry of Minerals, 16, 642–648.

Allan, D.R., Miletich, R., and Angel, R.J. (1995) A diamond-anvil cell for single-crystal X-ray diffraction studies to pressure in excess of 10 GPa. Reviews of Scientific Instruments, 67, 840–842.

Angel, R.J, Allan, D.R., Miletich, R., and Finger, L.W. (1997) The use of quartz as an internal pressure standard in high pressure crystallography. Journal of Applied Crystallography, 30, 461–466.

Chen, G., Weidner, D.J., and Liebermann, R.C. (1997) P-V-v_p-v_s measurements in SAM85 on MgO single crystal to 8 GPa and 1600 K: Calculating absolute pressures from ultrasonic interferometry and X-ray diffraction data. EOS, 78.

Chen, G., Liebermann, R.C., and Weidner, D.J. (1998) Elasticity of single-crystal MgO to 8 Gigapascals and 1600 Kelvin. Science, 280, 1913–1916.

Chopelas, A. (1992) Sound velocities to very high compression. Earth and Planetary Science Letters, 114, 185–192.

Duffy, T.S., Hemley, R.J., and Mao, H.K. (1995) Equation of state and shear strength at multimegabar pressures: Magnesium oxide to 227GPa. Physical Review B 74(8), 1371–1374.

Jackson, I. and Niesler, H. (1982) The elasticity of periclase to 3 GPa and some geophysical implications. In S. Akimoto, and M.H. Manghnani, Eds., High Pressure Research in Geophysics. Advances in Earth and Planetary Sciences 12, 93–112.

Karki, B.B., Stixrude, L., Clark, S.J., Warren, M.C., Ackland, G.J., and Crain, J. (1997) Structure and elasticity of MgO at high pressure. American Mineralogist, 82, 51–60.

Merrill, L. and Bassett, W.A. (1974) Miniature diamond anvil pressure cell for single crystal x-ray diffraction studies. Reviews of Scientific Instruments, 45, 290–294.

Piermarini, G.J., Block, S., and Barnett, J.D. (1973) Hydrostatic limits in liquids and solids to 100 kbar. Journal of Applied Physics, 44, 5377–5382.

Piermarini, G.J., Block, S., Barnet, J.D., and Forman, R.A. (1975) Calibration of the pressure dependence of the R_1 ruby fluorescence line to 195 kbar. Journal of Applied Physics, 46, 2774–2780.

Shen, A.H., Reichmann, H.J., Chen, G., Angel, R.J., Bassett, W.A., and Spetzler, H. (1998) GHz ultrasonic interferometry in a diamond anvil cell: P-wave velocities in periclase to 4.4 GPa and 207°C. In Murli H. Manghnani and Takehiko Yagi, Eds., Properties of earth and planetary materials at high pressure and temperature, p. 71–77. Geophysical Monograph Series, 101.

Sinogeikin, S.V. and Bass, J.D. (1998) Single crystal elasticity of synthetic pyrope and MgO by Brillouin scattering to 20 GPa. EOS supplement, AGU Spring meeting, May 26–29, Boston, Massachusetts.

Spetzler, H.A., Chen G., Whitehead, S., and Getting, I.C. (1993) A new ultrasonic interferometer for the determination of equation of state of sub-millimeter single crystals. PAGEOPH, 141, 341–373.

Spetzler, H., Shen, A., Chen, G., Herrmannsdoerfer, G., Schulze, H., and Wei-gel, R. (1996) Ultrasonic measurements in a diamond anvil cell. Physics of the Earth and Planetary Interiors, 98, 93–99.

Spetzler, H.A. and Yoneda, A. (1993) Performance of the complete travel-time equation of state at simultaneous high pressure and temperature. PAGEOPH, 141, 379–392.

Yoneda, A. (1990) Pressure derivatives of elastic constants of single crystal MgO and Mg Al_2O_4. Journal of Physics of the Earth, 38, 19–55.

MANUSCRIPT RECEIVED JUNE 10, 1998
MANUSCRIPT ACCEPTED AUGUST 7, 1998
PAPER HANDLED BY ANNE M. HOFMEISTER